

Synthesis and characterization of CdTe/CdS and CdTe/CdSe core/shell type-II quantum dots in a noncoordinating solvent

Jia-Yaw Chang¹, Shiuann-Ren Wang and Cheng-Hsien Yang¹

Nanopowder and Thin Film Technology Center, Industrial Technology Research Institute, 31 Gongye 2nd Road, Annan District, Tainan City, Taiwan 709, Republic of China

E-mail: jychang@itri.org.tw and jasonyang@itri.org.tw

Received 22 March 2007, in final form 13 June 2007

Published 27 July 2007

Online at stacks.iop.org/Nano/18/345602

Abstract

A synthetic route to CdTe/CdS and CdTe/CdSe core/shell type-II quantum dots in noncoordinating solvents (1-octadecene) was obtained. The results showed redshift in the emission spectra of CdTe/CdS and CdTe/CdSe compared with the CdTe core nanocrystals. This phenomenon is believed to indicate the formation of core/shell nanostructures. Transmission electron microscopy and powder x-ray diffraction were also consistent with nanocrystals containing a core of nearly monodisperse CdTe with CdS or CdSe capping. The photoluminescence quantum yield was enhanced by epitaxial growth of CdS or CdSe shells. Stepwise increasing concentration of sulfur or selenium monomers into the CdTe core solution allowed the examination of monomer activities, which are very relevant for synthesizing core/shell quantum dots.

1. Introduction

The unique and novel size-dependent properties displayed by semiconductor nanocrystals have initiated the current worldwide intense research on nanomaterials. Over the past two decades, great efforts have been put into the synthesis of highly fluorescent II–VI semiconductor nanocrystals [1–4]. The nanocrystals show great promise for use in various applications, such as biological fluorescence labelling [5–7], solar cells [8, 9] and organic/inorganic light emitting devices [10, 11] because quantum confinement provides molecular-like discrete energy levels and different colour emissions can be tuned by simply varying the size of the nanocrystals. Passivating surface nonradiative recombination sites of semiconductor nanocrystals with higher bandgap inorganic shells has been shown to improve photoluminescence (PL) quantum yields (QYs) and make the nanocrystals more robust than organically passivated ones [12, 13]. Compared to type-I quantum dots (QDs), type-II QDs have both valence and conduction bands of the core that are either

both lower or higher than those of the shell. The spatial separation of charge carriers and confinement leads to several characteristic differences from type-I QDs. Similar to staggered quantum wells, photoexcitation of type-II QDs results in charge separation of one type charge carrier in the core and the opposite sign charge carrier in the shell. Type-II QDs also provide interesting opportunities for tuning carrier–carrier interactions in structures, which is an important capability for such applications as lasing [14, 15], nonlinear optics [16, 17] and photovoltaic cells [18, 19], utilizing carrier multiplication. Of the various types of type-II QDs [20–24], the cadmium system has been the most intensively studied because of its quantum confinement effects and size-dependent photoemission characteristics. CdTe nanocrystals are expected to show a stronger quantum confinement and enhanced nonlinear optical properties [25].

In this report, the growth of CdTe nanocrystal cores with appropriate sizes are examined and narrow size distributions for overcoating these cores with CdS and CdSe in a noncoordinating solvent (1-octadecene). CdS and CdSe were chosen as the shell materials because of their small lattice

¹ Authors to whom any correspondence should be addressed.

mismatch (11.5% and 7.1%, respectively) [26, 27], which facilitates the epitaxial growth of the shell around CdTe cores. Moreover, both their lower valence and conduction gaps aid confinement of one carrier on the core and the other on the shell after photoexcitation. By exploring the effects of shell precursor concentration and the rate of precursor addition, the conditions for shell growth which do not yield substantial nucleation of nanocrystals of the shell semiconductor were optimized, while still minimizing the Ostwald ripening process. Stepwise increasing concentration of sulfur or selenium monomers into the CdTe core solution allowed the examination of how core/shell QDs are influenced by monomer activities.

2. Experimental section

2.1. Materials

Cadmium oxide (CdO, 99.99%) and sulfur (S, 99.98%) were purchased from Sigma. Tellurium (Te, 99.98%), 1-octadecene (ODE, 90%) and oleic acid (OA, 90%) were purchased from Aldrich. Octadecylamine (ODA, 97%) and trioctylphosphine (TOP, 90%) were purchased from Fluka. Selenium (Se, 99.5%) was purchased from Riedel-deHaen. All organic solvents were purchased from EM Sciences and all chemicals were used directly without any further purification.

2.2. Synthesis of CdTe core QDs

CdTe core nanocrystals were prepared via a modified literature method [28, 29]. Cadmium (Cd) precursors were prepared by adding 26 mg of CdO, 1.2 ml of OA and 20 ml of ODE to a three-neck flask clamped in a heating mantle. The mixture was heated to about 280 °C under argon flow and resulted in a colourless clear solution, which was then cooled to 200 °C for reaction. At this temperature, 1 ml of the Te injection precursors, which were made by dissolving 42.2 mg of Te in 0.8 ml TOP and diluted with 5 ml of ODE, was taken to quickly inject into this hot solution for 30 min. All steps in the reactions were carried out under argon atmosphere. An equal volume mixture of CHCl₃/CH₃OH (1:2) was used as the extraction solvent to separate the nanocrystals from byproducts and unreacted precursors. The as-prepared CdTe solution can be precipitated with acetone by centrifugation.

2.3. Synthesis of CdTe/CdS and CdTe/CdSe core/shell QDs

CdTe/CdS or CdTe/CdSe core/shell type-II QDs were obtained by a two-step synthetic procedure. 20 ml of the CdTe core solution (containing 7.2×10^{-2} mg, 3×10^{-4} mmol of CdTe QDs in ODE) and 5 ml of ODA were mixed together and heated to 250 °C. Cd monomer (0.04 M) was prepared by dissolving CdO (61.5 mg) in OA (1.3 ml) and ODE (10.8 ml) at 280 °C. The S and Se monomers (0.04 M) were prepared in ODE at 200 and 300 °C, respectively. Each clear monomer was obtained under an argon flow and allowed to cool to room temperature. Equal volume amounts of the Cd and S (or Se) monomers were mixed for preparing Cd-S (or Cd-Se) injection monomers and added dropwise to the vigorously stirred 25 ml core solution at 250 °C via a syringe pump (KdsScientific KDS230, USA) at a flow rate of 50 $\mu\text{l min}^{-1}$.

After the addition was complete, the reaction mixture was cooled to room temperature. Finally, the CdTe/CdS or CdTe/CdSe core/shell type-II QDs were precipitated by the addition of acetone, then separated, and finally redispersed for further processing.

2.4. Characterization

The nanocrystal solutions were dropped onto copper grids with carbon support by slowly evaporating the solvent in air at room temperature. The ultra structure of the nanocrystals was examined using transmission electron microscopy (TEM) (Philips, Tecnai G2 20 S-TWIN) with an LaB₆ type filament at an operating voltage of 200 kV. X-ray diffraction patterns were recorded using powder x-ray diffraction measurements (XRD, Rigaku D/max-b) using Cu K α radiation. PL spectroscopy investigations were carried out on a fluorescence spectrophotometer FL 150 (Labguide Corp., Taiwan) using a 150 W xenon lamp as the excitation source. The PL QYs of QDs were estimated following the procedure of [30] by comparison with Rhodamine 6G in ethanol, assuming its PL QYs as 95%.

3. Results and discussion

CdTe core QDs were prepared by the injection of a 'cold' (room temperature) solution of precursor molecules into hot liquid ODE (200 °C) with an appropriate amount of OA as ligand using a modified 'hot-injection' method [29]. The precursor solution consisted of Te in ODE. According to classical nucleation theory [31, 32], the following two expressions represent the crystal nucleation rate per unit volume, J , and the activation energy of homogeneous nucleation, ΔG :

$$J = A \exp(-\Delta G/kT) \quad (1)$$

$$\Delta G = -\frac{4}{V}\pi r^3 kT \ln(S) + 4\pi r^2 \gamma. \quad (2)$$

In the expressions above, V is the molecular volume of the precipitated species, k is the Boltzmann constant, T is the absolute temperature, S is the saturation ratio, γ is the surface energy per unit surface area and r is the radius of the nuclei. The radius of the critical nuclei is obtained from $d\Delta G/dr = 0$:

$$r_c = \frac{2V\gamma}{3kT \ln(S)} \quad (3)$$

where ΔG_v is a negative quantity.

The critical radius r_c represents the minimum size of a stable nucleus. Particles smaller than r_c will dissolve while particles bigger than r_c will grow to achieve a reduction in the free energy. Equation (3) explains the formation of critical nuclei necessary for the formation of CdTe nanoparticles. This 'hot-injection' method leads to the instantaneous formation of nuclei and Te precursor concentration is depleted due to growth, with the critical size becoming larger than the average size present. Figure 1 shows the emission spectra (normalized to the first emission maximum) of CdTe QDs taken at different time intervals for a reaction temperature of 200 °C. At the times indicated, a sample was taken

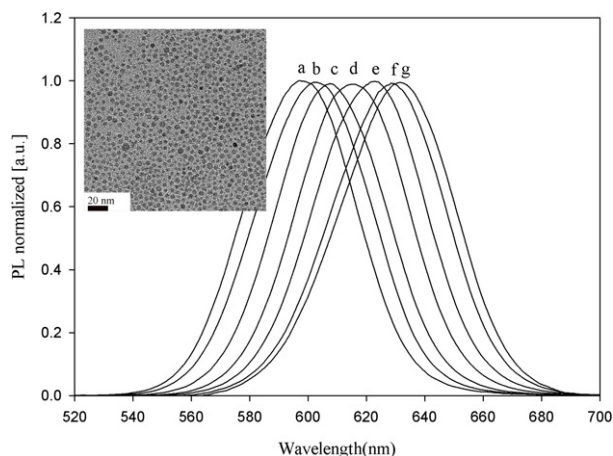


Figure 1. Normalized PL spectra of CdTe QDs taken from the same solutions, as a function of time: (a) 0.5 min, λ_{max} : 596 nm; (b) 1.0 min, λ_{max} : 602 nm; (c) 2.5 min, λ_{max} : 607 nm; (d) 5.0 min, λ_{max} : 614 nm; (e) 10 min, λ_{max} : 622 nm; (f) 30 min, λ_{max} : 629 nm; (g) 60 min, λ_{max} : 630 nm after injection of a Te precursor. The excitation wavelength for the PL spectra is 400 nm. The inset shows the TEM image of CdTe QDs after a precursor injection of 30 min.

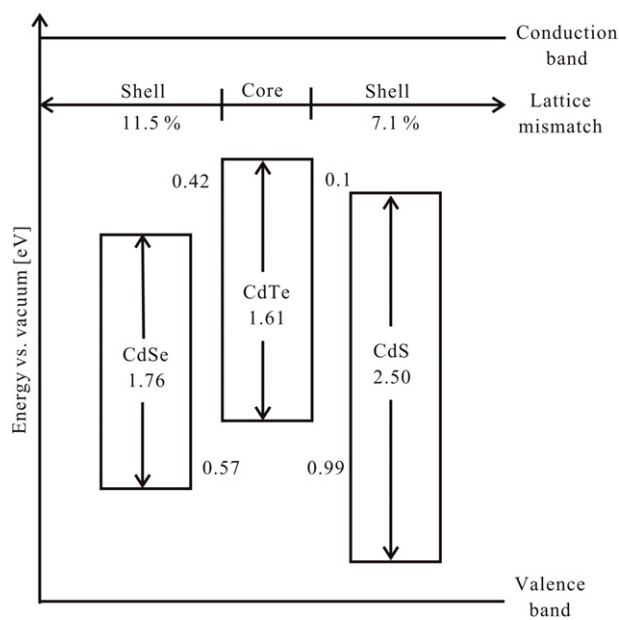


Figure 2. Bulk values of the band-edge position and energetic bandgaps for CdTe/CdS and CdTe/CdSe core-shell type-II QDs. The band offsets and lattice mismatch (in %) are given relative to CdTe.

from the hot reaction mixture and diluted into 1.5 ml of chloroform. The emission peaks of CdTe QDs ranged from 596 to 630 nm, and the corresponding full width at half-maximum (FWHM) of the band-edge luminescence was maintained between 52 and 55 nm, indicating that relatively monodispersed particles were obtained. The PL peak shifted to longer wavelengths with increasing CdTe sizes as a consequence of quantum confinement. The CdTe QDs in the inset of figure 1 indicate that monodispersed core nanocrystals formed good and well-ordered two-dimensional superlattices after a precursor injection of 30 min.

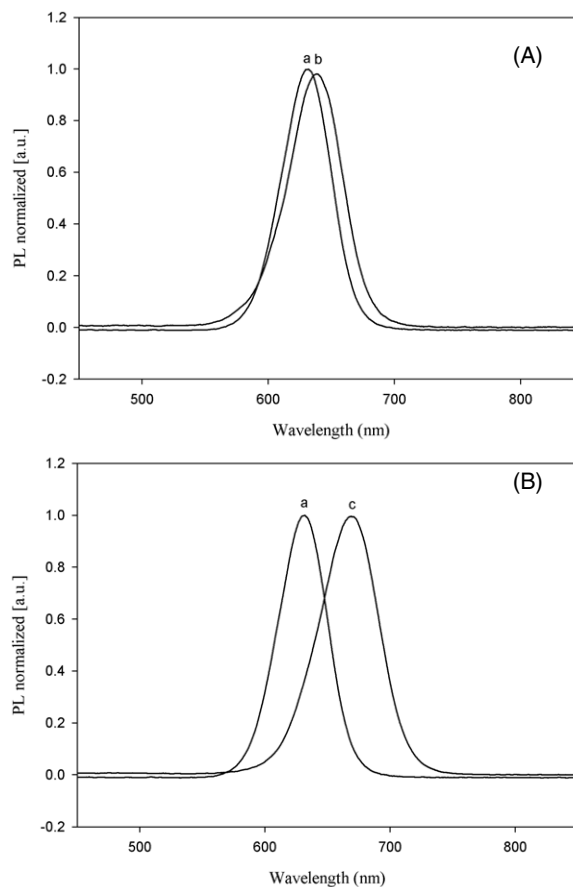


Figure 3. Normalized PL spectra for (A) CdTe/CdSe and (B) CdTe/CdS compared with the same CdTe core QDs.

Figure 2 presents the band-edge positions and bandgaps of bulk CdSe, CdTe and CdS [33]. From the diagram, it can be inferred that CdTe has the higher valence and conduction bands than CdS and CdSe for synthesizing type-II QDs. In addition, the small lattice mismatch between CdTe and CdS (or CdSe) is 11.5% (or 7.1%), which allowed an epitaxial growth of the shell around the core. A two-step synthetic procedure was used to produce CdTe/CdS and CdTe/CdSe type-II core-shell QDs. As shown in figure 1, the emission spectrum of CdTe QDs did not show any noticeable change when the system was heated at 200 °C for at least 30 min. CdTe QDs in this condition were further chosen as core QDs for passivating with CdS or CdSe on the outermost surface. Typically, a growth temperature of 250 °C for Cd-S and Cd-Se injection monomers was used because this temperature was found to be optimal [34]. Slow addition of the Cd-S or Cd-Se injection monomers at low concentrations ensured that most of the CdS or CdSe grow heterogeneously onto existing CdTe core QDs instead of undergoing homogeneous nucleation. To prepare the shell growth, 0.04 M Cd-S or Cd-Se injection monomers were added dropwise to the core solution via a syringe pump at a flow rate of 50 $\mu\text{l min}^{-1}$. The emission spectra of CdTe cores before overcoating and the corresponding CdTe/CdS and CdTe/CdSe core-shell QDs emission spectra after overcoating are displayed in figure 3. However, the results show a redshift of CdTe emission peak wavelength from 630 to 637 nm and at

671 nm after coating with CdSe and CdS, respectively, under the same injection amounts ($250 \mu\text{l}$).

To examine the monomer activities of CdSe and CdS shell growth on CdTe core QDs, Cd-S and Cd-Se injection monomers were separately added to a colloidal solution of CdTe core QDs with the same injection rate and concentration by means of a syringe pump. The immediate and significant redshift of the emission spectra after growth of the CdS and CdSe shells indicated that the resulting nanocrystals are both core/shell QDs, as shown in figure 4. The systematic redshift of the bandgap with the shell growth results from the extension of the carrier wavefunction into the shell region. The insets in figure 4 illustrate the corresponding evolution of PL QYs for these core/shell QDs as a function of injection time at a flow rate of $50 \mu\text{l min}^{-1}$. Within the CdSe shell thickness explored in this work, the PL QY of the core/shell QDs starts at 4.9% for 5 min of injection time and increases to 26.4% for 90 min of injection time as the CdSe shell thickness increased. Compared to CdTe/CdSe, the PL QY of CdTe/CdS core/shell QDs reaches a maximum value (27.4%) after 5 min and drops significantly with increased addition of Cd-S injection monomers. The emission of QDs is dependent upon the QDs size due to the quantum confinement effect, which only occurs when the size of the nanostructure is of the order of the exciton Bohr radius. However, the PL QY of CdTe/CdS is completely lost after 60 min. This result indicates that an apparently high tendency of the surrounding CdS shell to be preferentially grown on CdTe core QDs accompanied by the uncontrollable growth of particles, which may be responsible for the suppression of the PL QY. From figure 4, it can also be inferred that the epitaxial grown core/shell structure of the resulting nanocrystals can be determined using the S and Se monomer activity. For example, figure 4 shows that initially the position of the PL band of core/shell QDs is at 630 nm after the injection of CdS or CdSe precursors for 2.5 min. Due to CdS having a broader bandgap than CdSe (figure 2), the formation CdS shell on the CdTe will effectively passivate the CdTe surface and give rise to a large increase in PL intensity. After the addition of 1.5 ml of Cd-Se injection monomers (0.04 M), the emission features showed a peak maximum at 660 nm, as shown in figure 4(A) (d). The redshift of the emission spectra accompanied by a broadening of the size distribution such as the PL FWHM is about 50 nm (figure 4(A) (d)) and increases up to 69 nm (figure 4(A) (f)). The increase of PL FWHM in figure 4(A) (f) indicates that an Ostwald ripening stage may occur while Cd-Se monomers are continuously added and prolong the reaction time. This would allow for easier dissolution of some particles and growth of others. In addition, larger particles will emit longer wavelengths due to reduction in quantum confinement. When 0.25 ml of injection volume of Cd-S precursors (0.04 M) was added into the core reaction solution, the PL peak occurred at 680 nm (figure 4(B) (b)) and the PL intensity reached its maximum value when the thickness of the CdS shell increased to a critical threshold (the optimum thickness). Afterward, the PL intensity declined, accompanied by a broader PL emission while continuing to increase the volume of Cd-S injection monomers. From the above discussion, experimental results suggest that, instead of monomer concentrations, monomer activity (S or Se) is a more relevant term for synthesizing core/shell QDs. CdS shells are more preferential grown on

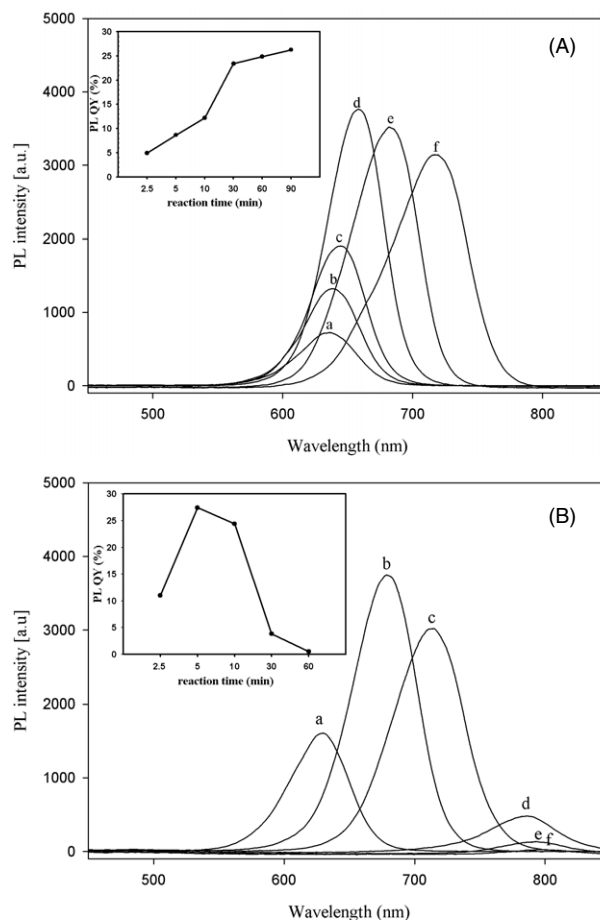


Figure 4. Evolution of the photoluminescence spectra taken from the (A) CdTe/CdSe and (B) CdTe/CdS core/shell solutions, as a function of time: (a) 2.5 min, (b) 5 min, (c) 10 min, (d) 30 min, (e) 60 min and (f) 90 min after adding (A) 0.04 M Cd-Se and (B) 0.04 M Cd-S injection monomers at a flow rate of $50 \mu\text{l min}^{-1}$. The PL QY (inset) is charted as a function of injection time.

CdTe core QDs than CdSe shells but fast kinetic growth rates make it difficult to control the epitaxial growth of the core/shell nanostructure.

Since the CdTe/CdSe and CdTe/CdS core/shell QDs were prepared from the same batch of the CdTe core QDs, the CdSe and CdS shell thicknesses can be estimated by the subtraction of the core size from that of the prepared core/shell particles. High-resolution TEM (HRTEM) images of CdTe, CdTe/CdSe and CdTe/CdS QDs synthesized in these systems are shown in figure 5, along with the histograms of size distribution on the right-hand side of each TEM image. The clear lattice plane observations are indicative of relatively good crystallinity. Figure 5 illustrates TEM images for CdTe core QDs with diameters of 3.4 nm (figure 5(A)) and CdTe/CdSe core/shells QDs with average diameters of 4.5 nm after the addition of 1.5 ml injection solutions of Cd-Se monomers (figure 5(B)). The average diameters of the 680 nm emitting CdTe/CdS core/shell QDs, as measured by TEM (figure 5(C)), are 5.3 nm after the addition of 0.25 ml injection solutions of Cd-S monomers. After adding 1.5 ml of Cd-S injection monomers, the average diameters of CdTe/CdS core/shell QDs increased from 5.3 to 11.2 nm, as shown in figure 4(D). The

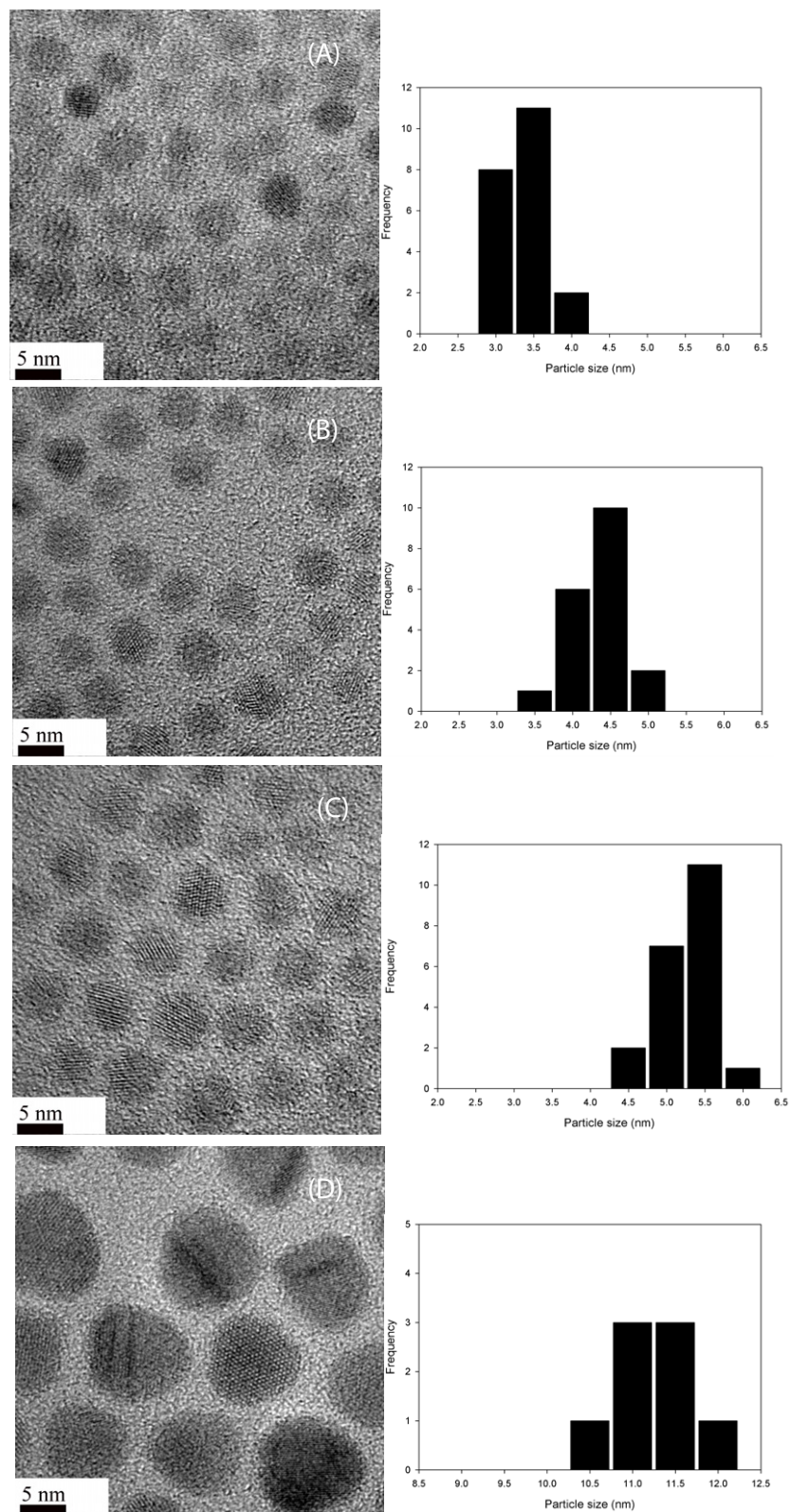


Figure 5. HRTEM images of plain CdTe core QDs and the corresponding core/shell nanocrystals with different CdS and CdSe shells but identical cores: (A) CdTe core QDs, (B) CdTe/CdSe with the addition of 1.5 ml of Cd–Se injection precursors, (C) CdTe/CdS with the addition of 0.25 ml of Cd–Se injection precursors and (D) CdTe/CdS with the addition of 1.5 ml of Cd–S injection precursors. The histograms show particle size distributions on the right-hand side of each TEM image.

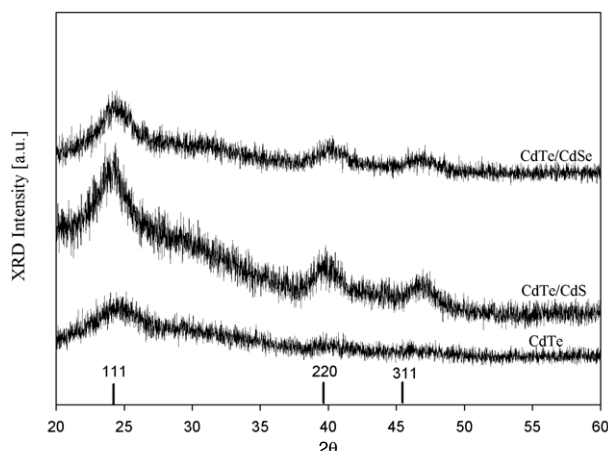


Figure 6. Powder x-ray diffraction patterns from CdTe, CdTe/CdS and CdTe/CdSe QDs.

mismatch of the lattice constants between core (CdTe) and shell (CdSe and CdS) are 7.1% and 11.1%, which are both too small to allow the resolution of the core and shell individually via the difference in the lattice orientations using TEM.

To further characterize the core/shell nanostructures, CdTe, CdTe/CdSe and CdTe/CdS were examined by powder XRD. After passivating CdS or CdSe shells, the diffraction pattern of CdTe moved slightly toward higher angles, which supports the formation of CdS or CdSe shells on CdTe. Figure 6 compares the diffraction patterns of CdTe cores with CdTe/CdS and CdTe/CdSe core/shells. Three diffraction peaks corresponding to the {111}, {200} and {311} lattice planes of the CdTe cores match those of the bulk CdTe cubic (zinc blende) peaks. The peaks are broadened because of the finite size of the nanocrystals. Upon the growth of the CdS or CdSe shell, peak positions shift to higher scattering angle, towards the positions of the bulk CdS or CdSe zinc blende peaks. In addition, substantial narrowing of the diffraction peaks is observed as demonstrated for the (111), (200) and (311) peaks shown in figure 6. The narrowing results from an increase of the crystalline domain size, indicating that shell growth is epitaxial.

4. Conclusion

In conclusion, a simple and fast approach for growing CdTe/CdS and CdTe/CdSe core/shell type-II QDs in noncoordinating solvents has been shown. Experimental results suggest that, instead of monomer concentrations, monomer activity (S or Se) is a more relevant term for synthesizing core/shell QDs. CdS shells are more preferentially grown on CdTe core QDs than CdSe shells, but fast kinetic growth rates of CdS make it difficult to control the epitaxial growth on the surface of CdTe core QDs. TEM and powder XRD are also consistent with nanocrystals containing a core of nearly monodispersed CdTe with a CdS or CdSe capping.

Acknowledgments

The authors gratefully acknowledge the financial support from the Taiwan Research Grant Council. We are indebted to

Professor Yong-Chien Ling (National Tsing Hua University, Taiwan) for his encouragement.

References

- [1] Murray C B, Norris D J and Bawendi M G 1993 *J. Am. Chem. Soc.* **115** 8706
- [2] Peng Z A and Peng X 2001 *J. Am. Chem. Soc.* **123** 183
- [3] Yu W W, Qu L, Guo W and Peng X 2003 *Chem. Mater.* **15** 2854
- [4] Manna L, Scher E C and Alivisatos A P 2000 *J. Am. Chem. Soc.* **122** 12700
- [5] Chan W C W and Nie S 1998 *Science* **281** 2016
- [6] Mattoussi H, Mauro J M, Goldman E R, Anderson G P, Sundar V C, Mikulec F V and Bawendi M G 2000 *J. Am. Chem. Soc.* **122** 12142
- [7] Ma J, Chen J Y, Guo J, Wang C C, Yang W L and Cheung N H 2006 *Nanotechnology* **17** 5875
- [8] Colvin V L, Schlamp M C and Alivisatos A P 1994 *Nature* **370** 354
- [9] Dabbousi B O, Onitsuka O, Bawendi M G and Rubner M F 1995 *Appl. Phys. Lett.* **66** 1316
- [10] Coe S, Woo W K, Bawendi M and Bulovic V 2002 *Nature* **420** 800
- [11] Tessler N, Medvedev V, Kazes M, Kan S and Banin U 2002 *Science* **295** 1506
- [12] Dabbousi B O, Rodriguez-Viejo J, Mikulec F V, Heine J R, Mattoussi H, Ober R, Jensen K F and Bawendi M G 1997 *J. Phys. Chem. B* **101** 9463
- [13] Seker F, Meeker K, Kuech T F and Ellis A B 2000 *Chem. Rev.* **100** 2505
- [14] Ivanov S A, Nanda J, Piryatinski A, Achermann M, Balet L P, Bezel I V, Anikeeva P O, Tretiak S and Klimov V I 2004 *J. Phys. Chem. B* **108** 10625
- [15] Klimov V I, Mikhailovsky A A, Xu S, Malko A, Hollingsworth J A, Leatherdale C A, Eisler H J and Bawendi M G 2000 *Science* **290** 314
- [16] Petruska M A, Malko A V, Voyles P M and Klimov V I 2003 *Adv. Mater.* **15** 610
- [17] Kraebel B, Malko A, Hollingsworth J and Klimov V I 2001 *Appl. Phys. Lett.* **78** 1814
- [18] Colvin V L, Schlamp M C and Alivisatos A P 1994 *Nature* **370** 354
- [19] Dabbousi B O, Onitsuka O, Bawendi M G and Rubner M F 1995 *Appl. Phys. Lett.* **66** 1316
- [20] Xie R, Zhong X and Basche T 2005 *Adv. Mater.* **17** 2741
- [21] Kim S, Fisher B, Eisler H J and Bawendi M 2003 *J. Am. Chem. Soc.* **125** 11466
- [22] Chou P T, Chen C Y, Cheng C T, Pu S C, Wu K C, Cheng Y M, Lai C W, Chou Y H and Chiu H T 2006 *ChemPhysChem* **7** 222
- [23] Yu K, Zaman B, Romanova S, Wang D and Ripmeester J A 2005 *Small* **1** 332
- [24] He Y, Lu H T, Sai L M, Lai W Y, Fan Q L, Wang L H and Huang W 2006 *J. Phys. Chem. B* **110** 13370
- [25] Padilha L A, Neves A A R, Cesar C L, Barbosa L C and Brito Cruz C H 2004 *Appl. Phys. Lett.* **85** 3256
- [26] He Y, Lu H T, Sai L M, Lai W Y, Fan Q L, Wang L H and Huang W 2006 *J. Phys. Chem. B* **110** 13370
- [27] Sze S M 1981 *Physics of Semiconductor Devices* (New York: Wiley) pp 848–9
- [28] Yu W W and Peng X 2002 *Angew. Chem. Int. Edn* **41** 2368
- [29] Donega C M, Liljeroth P and Vanmaekelbergh D 2005 *Small* **1** 1152
- [30] Demas J N and Crosby G A 1971 *J. Phys. Chem.* **75** 991
- [31] Turnbull D J and Fisher J C 1949 *J. Chem. Phys.* **17** 71
- [32] Oxtoby W 1998 *Acc. Chem. Res.* **31** 91
- [33] Wei S H, Zhang S B and Zunger A 2000 *J. Appl. Phys.* **87** 1304
- [34] Li J J, Wang Y A, Guo W, Keay J C, Mishima T D, Johnson M B and Peng X 2003 *J. Am. Chem. Soc.* **125** 12567